Lab on a Chip

PAPER

View Article Online
View Journal | View Issue

Cite this: *Lab Chip*, 2015, **15**, 3723

Patchiness in a microhabitat chip affects evolutionary dynamics of bacterial cooperation†‡

Edward W. Tekwa,*[a] Dao Nguyen,[b] David Juncker,[c] Michel Loreau[d] and Andrew Gonzalez[a]

Received 24th May 2015,
Accepted 24th July 2015

DOI: 10.1039/c5lc00576k

www.rsc.org/loc

Localized interactions are predicted to favour the evolution of cooperation amongst individuals within a population. One important factor that can localize interactions is habitat patchiness. We hypothesize that habitats with greater patchiness (greater edge-to-area ratio) can facilitate the maintenance of cooperation. This outcome is believed to be particularly relevant in pathogenic microbes that can inhabit patchy habitats such as the human respiratory tract. To test this hypothesis in a simple but spatially controlled setting, we designed a transparent microhabitat chip (MHC) with multiple patchiness treatments at the 100 micron scale. The MHC is a closed system that sustains bacterial replication and survival for up to 18 hours, and allows spatial patterns and eco-evolutionary dynamics to be observed undisturbed. Using the opportunistic pathogen *Pseudomonas aeruginosa*, we tracked the growth of wild-type cooperators, which produce the public good pyoverdin, in competition with mutant defectors or cheaters that use, but do not produce, pyoverdin. We found that while defectors on average outperformed cooperators in all habitats, habitat patchiness significantly alleviated the ecological pressure against cooperation due to defection, leading to coexistence. Our results confirmed that habitat-level spatial heterogeneity can be important for cooperation. The MHC enables novel experiments, allows multiple parameters to be precisely varied and studied simultaneously, and will help uncover dynamical features of spatial ecology and the evolution of pathogens.

1. Introduction

The evolution of cooperation has driven the rise of biological complexity.[1,2] But, because cooperation is costly, it is not necessarily evolutionarily viable unless the benefit of cooperation tends to be directed toward cooperators. The non-uniform spatial distribution of individuals is one of the most important factors favouring the evolution of cooperation.[3–10] As individuals become more clustered, the benefit of cooperation can be preferentially bestowed on cooperators, making cooperation viable, either in the traditional evolutionary sense—the frequency of cooperators is greater than for defectors[11]—or in an ecological sense—localized interactions are stabilizing and lead to coexistence.[12–14]

Spatial patchiness, or the ratio of edge-to-area,[15] characterizes the habitats of most organisms,[16] including bacteria.[17] It appears that patchiness can facilitate cooperation in bacteria,[18] likely because interactions become localized. Common bacteria such as *Pseudomonas aeruginosa* are opportunistic pathogens that live in the soil[19] and water,[20] and can colonize various parts of the patchy human respiratory tract.[21] The wild-type bacteria are cooperators that produce the siderophore pyoverdin, a diffusible extracellular iron-chelator responsible for bacterial iron uptake and growth[22] that is a form of public good. The production of a public good,[23,24] by definition, implies an individual behaviour that benefits the public or the wider population, so cooperation can have an important ecological effect. Interestingly, loss-of-function mutants, or defectors, often arise in the human host environment over time.[25–27] Thus, the evolutionary race between cooperators and defectors in patchy habitats is an important case for both general eco-evolutionary theory[18,28–30] and the study of infectious diseases.[31,32]

[a] *Department of Biology, McGill University, 1205 Dr. Penfield, Montreal, QC, H3A 1B1, Canada. E-mail: tek.wa.wong@mail.mcgill.ca*
[b] *Department of Medicine, McGill University, 1001 Decarie Blvd, Montreal, QC, H4A 3J1, Canada*
[c] *Biomedical Engineering Department, Genome Quebec Innovation Centre, and Department of Neurology and Neurosurgery, McGill University, 740 Dr. Penfield, Montreal, QC, H3A 0G1, Canada*
[d] *Centre for Biodiversity Theory and Modelling, Station d'Ecologie Expérimentale du CNRS, 09200, Moulis, France*

† Statement of authorship: EWT, AG, ML conceived the study. EWT designed and performed the experiment. DJ and AG contributed to the chip design and fabrication. DN and AG provided the bacteria strains and guidance on experimental design. EWT wrote the first draft, and all authors contributed substantially to revisions.

‡ Electronic supplementary information (ESI) available. See DOI: 10.1039/c5lc00576k

The traditional approach of emulating habitat structure and localized interaction has been through serial transfers of liquid subpopulations.[29,33] This approach imposed cyclical bottlenecks on population size[34,35] during transfers, and did not allow populations to form natural aggregates, since growth occurred in a relatively large-volume of well-mixed liquid. Larger beaker[36] and flow cell experiments[37] allowed for endogenous spatial pattern formation, but at much larger spatial scales where whole-population census is generally not feasible.

Various microfluidic devices[30,38–43] have been developed to emulate patchy microbial habitats, which afford the capacity to track individuals in space and time while minimizing sample volumes. These devices allowed detailed investigations of microbial movement, pattern formation, and interaction.[44] In particular, it was observed that in comparison to well-mixed test tube cultures, a microhabitat favoured the maintenance of cooperation.[18] However, these devices did not contain a systematic variation in habitat patchiness, and required substantial setup time. Building on these past innovations, we introduce a microhabitat chip (MHC) that is simple to fabricate and operate, reusable, and systematically varies habitat patchiness.

The MHC is a reusable poly(dimethyl)siloxane (PDMS) chip that contains 9 habitats with varying patchiness. Patchiness was achieved by fragmenting habitats at 100 micron scales. We used simplicity and functionality as guiding principles[45] to focus on acquiring accurate individual-level spatiotemporal data for entire habitats. The PDMS elastomer layer seals with an optical cover slip to create an enclosed environment for bacteria to spatially self-organize with minimal disturbance. We investigate whether three habitat patchiness treatments affect the evolution of pyoverdin[46,47] producers, and therefore the growth and equilibrium densities of cooperators and defectors in *P. aeruginosa*. The wild-type cooperators and mutant defectors were genetically engineered to emit green or red fluorescence, so that their population size and spatial location can be accurately quantified by confocal microscopy.

We performed monoculture and mixed culture experiments to ascertain whether habitat patchiness affects maximum growth rates and equilibrium densities of these populations. We found that while defectors on average outperformed cooperators in all habitats, and are thus more likely to achieve dominance, patchiness contributed to the ecological coexistence of cooperators and defectors.

2. Methods

The MHC (Fig. 1) contains 9 treatments of habitat patchiness, with each habitat ranging from 1400 μm to 2670 μm in diameter, and 10 or 20 μm in depth. Each habitat takes the shape of a ring or a network of patches, representing a range of continuous and patchy treatments with various theoretically motivated topologies (see Fig. 2 and ESI† Fig. S1 for specifications). Here we focus on three treatments that

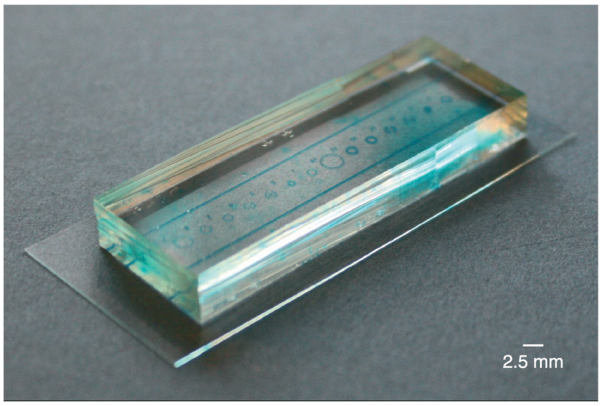

Fig. 1 The microfluidic device contains 14 habitats and 9 variations (some are duplicated). Habitats were dyed blue for visualization. The elastomer (PDMS) layer was pressed onto a 60 mm × 24 mm glass cover slip after inoculation to create a sealed device. The confocal microscope acquired images through the thin cover slip.

transition from continuous to patchy (Fig. 2), which are 10 μm deep and 0.42 mm^2 in the main habitat area. At this depth, all bacteria are confined to a thin layer, which facilitates image acquisition. Habitat 1 represents the most continuous case, whereas habitat 2 represents an intermediary between the continuous and patchy cases. A central pillar is necessary in these habitats to prevent collapse due to aspect ratio constraints.[48] In habitat 3, 24 × 100 μm^2 corridors are introduced between 12 circular patches (210 μm diameter) to represent a patchy case with the simplest network topology (area including corridors is 0.45 mm^2). The edge-to-area ratios of the habitats are 0.011, 0.015, and 0.022 μm^{-1}, which represent an approximately linear increase in patchiness.[15] Compared to the size of *P. aeruginosa* (~1 μm diameter), the 100 micron scale patchiness treatments in the three habitats are large. On the other hand, an individual bacterium can theoretically traverse 100 μm in several seconds,[49] but slows down considerably in aggregates when spatially confined.[50] We expect that the chosen scale of patchiness treatments can affect eco-evolutionary dynamics. During experiments, the three habitats run in parallel. Other habitat treatments are shown in the ESI† Fig. S1, but no time-series data was acquired for these because of time constraints imposed by our image acquisition setup. We included these extra habitat treatments as references for future users.

A silicon mold with two spin-coated layers (to accommodate both 10 and 20 μm depth features) was produced using photolithography (McGill Nanotools Microfab). Polydimethylsiloxane (Sylgard 184 PDMS, Dow Corning) was poured onto the mold, cured, and detached to yield MHC replicates that are about 5 mm thick, and baked at 100 °C for at least 24 hours. To make the PDMS MHC hydrophilic, it was soaked in 0.01 N HCl at 80 °C for one hour, then plasma treated (modified after[41]). Finally, the MHC was autoclaved, and stayed in the sterilized water at room temperature until the experiment began. The MHC thus remained saturated with water, which mitigated drying during the experiment.

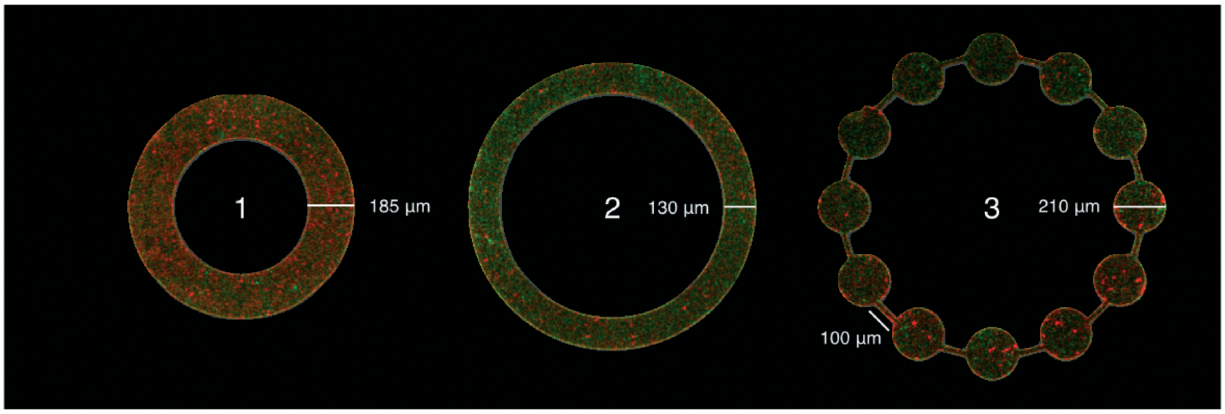

Fig. 2 Three habitat patchiness treatments. The habitats were inoculated with green cooperators and red defectors. Images shown were taken at T = 10 (about 10 hours after inoculation). The habitats are 10 μm deep and have diameters of 915, 1165 and 1405 μm. The corridors are 24 μm wide. The habitat areas are 0.42, 0.42, and 0.45 mm^2. The edge-to-area ratios, or patchiness measures, are 0.011, 0.015, and 0.022 μm^{-1}.

We used the common *P. aeruginosa* lab strain PAO1 as our wild-type cooperators, and an isogenic *pvdA* transposon mutant,[51] which is defective in producing the primary iron-chelating siderophore (pyoverdin), as defectors. The cooperator and defector strains were transformed with plasmids that constitutively expressed either the green fluorescent protein GFP (pMRP9-1 (ref. 52)) or the red mCherry (pMKB1 (ref. 53)).

In 8 independent experimental replicates for each of 3 culture conditions (cooperator monocultures, defector monocultures, mixed cultures at 1 : 1 initial ratio) in the MHC, the expression of GFP or mCherry in cooperators and defectors were alternated to average out fluorescence-dependent growth or measurement biases. Cultures were prepared overnight (16 hours) in LB media with antibiotic (250 μg ml^{-1} carbenicillin) at 37 °C in a shaker incubator. The overnight bacterial cultures were washed and diluted to an optical density (600 nm) of 0.005. The experimental media consisted of casamino acids (5 g with 0.005 M K_2HPO_4 and 0.001 M $MgSO_4$ per litre), 50 mM $NaHCO_3$ and 1 mg mL^{-1} human apo-transferrin to create an iron-limited environment where the cooperators' pyoverdin production should be beneficial.[29,46] 0.7 μL of the diluted culture was pipetted onto each of the habitat locations on the PDMS MHC (Fig. 1). The MHC was then carefully pressed onto a cover slip (24 × 60 mm #1.5H, Schott Nexterion), and excess liquid was wiped from the sides. By minimizing the amount of liquid used, the PDMS reversibly sealed to the glass for the duration of the

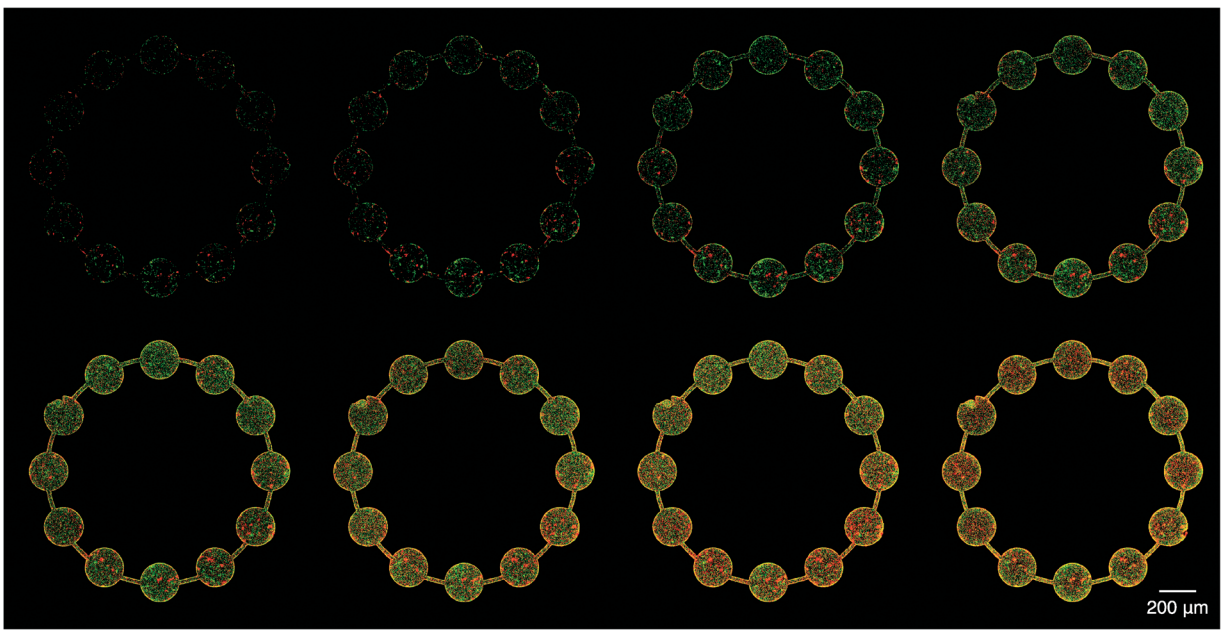

Fig. 3 Timed images of green cooperators and red defectors in a patchy habitat (T = 5 to 12 from top left to bottom right). For all figures, the time interval T is 57 minutes 18 seconds.

experiment without additional treatment. Three such MHCs were fitted into a 30 °C heat chamber (Chamlide TC, Live Cell Instrument) on the inverted robotic stage of a laser scanning confocal microscope (LSM 700, Zeiss) to allow for parallel experiments (two for monocultures and one for mixed culture). The chamber interior was lined with wet tissue papers and water wells to maintain chip moisture. Images covering the relevant habitats, with 5 *z*-slices covering a 20 μm slab, were acquired every 57 minutes and 18 seconds (the minimum acquisition time in our case) for 20 time points (Fig. 3). After an experiment, the MHC was disassembled and soaked in 70% ethanol, washed, and autoclaved for reuse. Each MHC can be used at least 10 times with no noticeable degradation.

The images were cropped to show only habitat and corridor areas (ImageJ 1.49). We then obtained the count and position of each individual bacterium at every time point (Imaris 7.6.0). Some biases were observed in comparing raw GFP and mCherry counts of the same strain in monocultures, and in comparing monocultures to mixed fluorescence cultures of the same strain. These biases were corrected through a calibration procedure (see ESI†).

The corrected counts were converted to densities X for each habitat, and the resulting time series were fitted to logistic growth curves using least-squares maximum likelihood (Matlab R2013a, eqn (1)):

$$\frac{dX_{i,S}}{X_{i,S}dt} = r_{i,S}\left(1 - X_{i,S}/K_{i,S}\right) \quad (1)$$

For a replicate of each strain i (cooperator or defector) in each culture condition S (monoculture or mixed culture), we estimated its maximum growth rate r and equilibrium density K. Note that we used the parameter K not as a carrying capacity, which would not make sense in a mixed culture involving both inter- and intra-strain competition and cooperation. Instead, we used K as an estimate of a strain's equilibrium density, since the logistic growth curve describes the trajectories of each strain well regardless of culture type and the length of individual time series (Fig. 4).

3. Results and discussion

In 8 biological replicates of each habitat and culture types (two monocultures and a mixed culture), bacteria replicated and survived for 12 to 18 hours. The mean initial density for each experiment was 0.0019 μm^{-2} (SE = 1.9×10^{-4}), and according to ANOVA there was no evidence of bias between culture type ($F_{2,66} = 3.0$, $p = 0.055$) or between habitats ($F_{1,66} = 0.72$, $p = 0.40$). For mixed cultures, according to ANOVA, cooperator and defector initial densities were not significantly different ($F_{1,45} = 0.091$, $p = 0.76$) and were not influenced by habitats ($F_{1,45} = 0.36$, $p = 0.55$), indications that

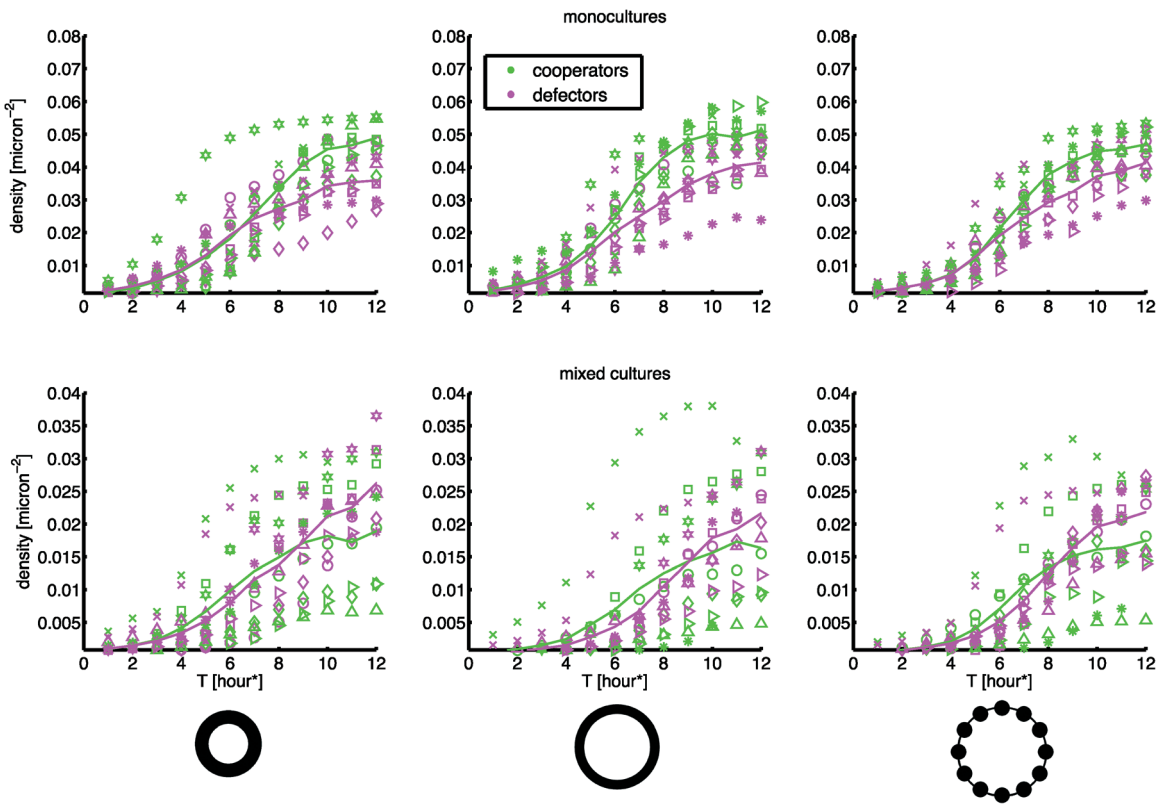

Fig. 4 Time series of cooperator and defector monocultures, and mixed cultures in three habitat patchiness treatments, as illustrated by icons at the bottom. Densities are expressed as individuals per micron squared. The different markers represent the 8 experimental replicates, and the line plots are averages for each strain at each time point. *Each time interval T is 57 minutes 18 seconds.

the experiments started at the desired 1 : 1 cooperator-defector ratios. All cooperator and defector populations demonstrated expected growth kinetics during the experimental time frame, with evidence of lag, log and stationary phases (by 10 hours, Fig. 4), characteristics of logistic growth curves. The equilibrium density estimates (K) represent strain populations that range from 2400 (cooperators in a mixed culture) to 38 000 (cooperators in a monoculture) individuals, or 5.6×10^8 to 9.0×10^9 individuals per mL.

We found that the maximum growth rate r (ESI† Fig. S3) was not significantly different in all cases according to ANOVA ($F_{3,87} = 2.2$, $p = 0.096$ for strain and culture type effect, $F_{1,87} = 0.090$, $p = 0.77$ for patchiness effect, and $F_{3,87} = 0.23$, $p = 0.88$ for interaction effect).

In monocultures, the equilibrium density K (ESI† Fig. S4) was significantly greater for cooperators than for defectors (ANOVA $F_{1,44} = 22$, $p = 2.9 \times 10^{-5}$), but was not significantly different across patchiness treatments ($F_{1,44} = 0.06$, $p = 0.81$); the interaction between strain and patchiness was not statistically significant either ($F_{1,44} = 3.2$, $p = 0.081$). In other words, cooperation enhanced population densities regardless of habitat patchiness. In mixed cultures, K was significantly lower for cooperators than for defectors ($F_{1,43} = 8.3$, $p = 0.0063$), but was not significantly different in terms of patchiness ($F_{1,43} = 0.0024$, $p = 0.96$) and the interaction between strain and patchiness ($F_{1,44} = 0.047$, $p = 0.83$). Thus, defectors significantly outperformed cooperators in all habitats, a result that was also found in well-mixed test tube cultures (see ESI†). This illustrates the cooperation dilemma,[24,54,55] where uniform cooperation provides the best outcome for the population, but is an evolutionarily inferior strategy.

We can further investigate the cooperation dilemma from an ecological perspective through the differences between monocultures and mixed cultures. Judging from monoculture equilibrium densities alone (K_{mono}), one may expect cooperators to be evolutionarily dominant over defectors (since $K_{\mathrm{mono,C}} > K_{\mathrm{mono,D}}$). If each strain grows in mixed cultures as if in monoculture, then the ratio $2K_{\mathrm{mix}}/K_{\mathrm{mono}}$ for each strain should be one.[56] The actual ratios, computed from bootstrapping, turned out to differ from one (box plots in Fig. 5). Note these ratios were plotted as estimated spreads instead of individual points, since they were derived statistics from unpaired experiments (by resampling with replacement the numerator and denominator 2000 times). For cooperators, $2K_{\mathrm{mix,C}}/K_{\mathrm{mono,C}}$ was less than one in all habitats, indicating that when evolutionarily challenged by defectors, they did not grow as well. Conversely, for defectors, $2K_{\mathrm{mix,D}}/K_{\mathrm{mono,D}}$ was greater than one in all habitats, meaning that they benefited from cooperators.

The habitat patchiness effects on the $2K_{\mathrm{mix}}/K_{\mathrm{mono}}$ ratios can be quantified as the slopes of bootstrapped linear regressions. By repeating the regression on the ratio computed from the resampling of K_{mix} and K_{mono} values with replacement 2000 times, we obtained the median regression slopes (lines in Fig. 5), and obtained distributions of regression slopes with which to calculate the following p values. We

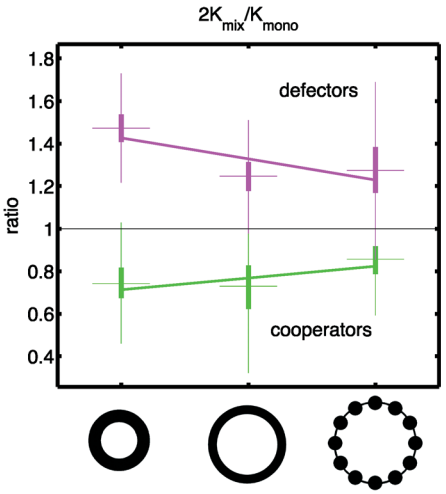

Fig. 5 The ratios of equilibrium densities (K) in mixed cultures (×2) over monocultures as estimated from bootstrapping for three habitats. If the interaction between cooperators and defectors has no effect on their equilibrium densities, the ratio should be 1. In the box plots, horizontal bars indicate medians, thick vertical bars (boxes) indicate 25th and 75th percentiles, and thin vertical bars indicate minima and maxima excluding outliers. From bootstrapped linear regressions, patchiness significantly increased the ratio for cooperators (green regression line, $p = 0.0075$), but marginally decreased the ratio for defectors (magenta regression line, $p = 0.16$).

found that patchiness did not affect the $2K_{\mathrm{mix,D}}/K_{\mathrm{mono,D}}$ ratio for defectors ($p = 0.16$). On the other hand, patchiness significantly increased the $2K_{\mathrm{mix,C}}/K_{\mathrm{mono,C}}$ ratio for cooperators ($p = 0.0075$). These trends suggest that with increased patchiness, the ecological pressure against the pyoverdin public good cooperation, stemming from the challenge by defectors, is alleviated. Moreover, as patchiness increases, the ratios $2K_{\mathrm{mix,C}}/K_{\mathrm{mono,C}}$ and $2K_{\mathrm{mix,D}}/K_{\mathrm{mono,D}}$ appear to approach one, so patchiness leads competing strains to grow as if in isolation. This effect is known in ecology as a spatial stabilizing effect, in that patchiness isolates strains such that they increasingly compete within strains rather than between strains, leading to coexistence regardless of how competitive each strain is relative to the other.[12–14]

Our experiment generated the first empirical evidence that a gradual increase in habitat patchiness, occurring at a scale much larger than the individual, can affect the evolution of cooperation and the coexistence of cooperators and defectors in bacteria. These results complement a previous microfluidic experiment,[18] which demonstrated the coexistence of bacterial cooperators and defectors in one microhabitat. The results are comparable to traditional test tube experiments, which by controlling serial transfer patterns, showed that spatial restrictions and artificially localized interactions can favour the evolution of cooperation.[29,33–35] Our MHC also provides an alternative to beaker[36] and flow cell experiments,[37] which study cooperative aggregates and biofilms at much larger spatial scales where whole-population census is generally not feasible.

We have overcome important challenges that are crucial for the use of microscale habitat devices in evolutionary

biology. The major obstacles to a wider uptake of microfluidic technologies are costly start-up equipment, complicated setup, and associated risks of error and contamination,[45] complexities that are not always geared to answer basic but outstanding eco-evolutionary questions. In creating a sealed chip that can run multiple replicates without pumps for 12–18 hours, we have enabled high-throughput spatial experiments with minimal setup time and cost. The runtime is an improvement over previous PDMS microhabitat devices,[38,39] and is much simpler to operate than devices requiring active nutrient flow.[30,40–42] Many aspects of the generated data, such as individual positions, population spatial distributions, and movement patterns can be further investigated, and would lead to a more comprehensive understanding of patchiness and individual-level clustering effects[57,58] than what our current analyses yielded. It is also possible to recover bacteria from the MHC at the end of experiments to detect *de novo* mutations through sequencing.[42] The simplicity of the MHC greatly facilitates running an entire eco-evolutionary experiment on a chip.

Some limitations exist with the MHC. Because of aspect ratio requirements with PDMS chambers,[48] it is not possible to create patches and habitats of any dimension. The enclosed system afforded by our design is simple and exhibits the familiar logistic growth of bacteria (Fig. 4). However, without serial transfer of bacteria into fresh medium, the system limits the possible duration of the experiment for the following reasons. PDMS facilitates gas exchange, but gradually absorbs liquid at the same time.[59] The sealed system also prevents nutrients from being replenished, but conversely minimizes the risks of external contamination. Lastly, the number of different strains that can be tracked simultaneously was limited by the number of fluorescent proteins (*e.g.* GFP, mCherry) distinguishable using our current setup, but additional fluorescent proteins are available.[60]

4. Conclusions

We demonstrated that a simple and reusable microfluidic chip can provide insights into the eco-evolutionary dynamics of *Pseudomoas aeruginosa*, a medically important pathogen. In the first microbial cooperation experiment with multiple spatial habitat treatments, we observed that mutant defectors are evolutionarily more competitive than wild-type cooperators that produce siderophores. However, the ecological pressure against cooperation due to defection is alleviated in increasingly patchy habitats, leading to continued coexistence (Fig. 5). The trends suggest that at patchiness levels higher than those we tested, competing strains may grow as if in isolation – a hypothesis that merits further investigations.

The results suggest that pathogenic bacteria in patchy habitats, such as the respiratory tract,[21] may be more cooperative in exploiting nutrient resources in comparison to a continuous habitat like a conventional test tube. Nevertheless, defectors, or loss-of-function mutants, can be expected to arise and co-exist with wild-type cooperators, as has been observed in patients with cystic fibrosis.[25–27] The simple chip design and operation should facilitate its uptake in ecological, evolutionary, and medical research, leading to novel experiments that complement existing studies on microbes in spatially complex environments.[18,29,37,42,61] Specifically, future experiments using our microhabitat chip can address how habitat patch size and corridor topology affect demography[62–64] and cooperation,[5,65] and how nutrient availability[66] interacts with patchiness to affect microbial community dynamics.[67]

Acknowledgements

EWT was supported by the Fonds Québécois de la Recherche sur la Nature et les Technologies and the Québec Centre for Biodiversity Science. ML was supported by the TULIP Laboratory of Excellence (ANR-10-LABX-41). AG and DJ were supported by the Canada Research Chair program and NSERC Discovery grants. DN was supported by a CFI Leaders Opportunity Fund (25636), a Burroughs Wellcome Fund CAMS award (1006827.01) and a CIHR salary award. M. Nannini created the silicon mold for the chip. G. A. McKay helped creating the GFP and mCherry strains in the study, and provided experimental guidance. We would like to thank M. R. Parsek and S. Moskowitz for generously providing the pMRP9-1 and pMKB1 plasmids, respectively.

References

1 J. Maynard Smith and E. Szathmáry, *The origins of life*, Oxford University Press, Oxford, 1999.
2 W. D. Hamilton, *J. Theor. Biol.*, 1964, **7**, 1–16.
3 S. Lion and M. van Baalen, *Ecol. Lett.*, 2008, **11**, 277–295.
4 J. A. Fletcher and M. Doebeli, *Proc. R. Soc. B*, 2009, **276**, 13–19.
5 C. E. Tarnita, H. Ohtsuki, T. Antal, F. Fu and M. A. Nowak, *J. Theor. Biol.*, 2009, **259**, 570–581.
6 F. Débarre, C. Hauert and M. Doebeli, *Nat. Commun.*, 2014, **5**, 3409.
7 D. S. Wilson, *Am. Nat.*, 1977, **111**, 157–185.
8 F. Rousset, *Genetic Structure and Selection in Subdivided Populations*, Princeton University Press, Princeton, NJ, 2004.
9 A. Gardner and S. A. West, *J. Evol. Biol.*, 2004, **17**, 1195–1203.
10 H. Celiker and J. Gore, *Trends Cell Biol.*, 2013, **23**, 9–15.
11 S. H. Rice, *Evolutionary Theory*, Sinauer, Sunderland, MA, 2004.
12 S. A. Levin, *Am. Nat.*, 1974, **108**, 207–228.
13 B. M. Bolker and S. W. Pacala, *Am. Nat.*, 1999, **153**, 575–602.
14 P. Chesson, *Annu. Rev. Ecol. Syst.*, 2000, **31**, 343–366.
15 P. A. Marquet, M.-J. Fortin, J. Pineda, D. O. Wallin, J. Clark, Y. Wu, S. Bollens, C. M. Jacobi and R. D. Holt, in *Patch dynamics*, ed. S. A. Levin, T. M. Powell and J. H. Steele, Springer-Verlag, New York, 1993, pp. 277–304.
16 S. A. Levin, *Ecology*, 1992, **73**, 1943–1967.
17 C. H. Ettema and D. A. Wardle, *Trends Ecol. Evol.*, 2002, **17**, 177–183.

18 F. J. H. Hol, P. Galajda, K. Nagy, R. G. Woolthuis, C. Dekker and J. E. Keymer, *PLoS One*, 2013, **8**, e77402.
19 S. K. Green, M. N. Schroth, J. J. Cho, S. K. Kominos and V. B. Vitanza-jack, *Appl. Microbiol.*, 1974, **28**, 987–991.
20 K. Botzenhart and G. Döring, in *Pseudomonas aeruginosa as an Opportunistic Pathogen*, Springer, US, 1993, pp. 1–18.
21 A. Folkesson, L. Jelsbak, L. Yang, H. K. Johansen, O. Ciofu, N. Høiby and S. Molin, *Nat. Rev. Microbiol.*, 2012, **10**, 841–851.
22 K. Poole and G. A. McKay, *Front. Biosci*, 2003, **8**, 661–686.
23 M. Olson, *The Logic of Collective Action*, Harvard University Press, Harvard, MA, 1965.
24 E. Ostrom, *J. Econ. Perspect.*, 2000, **14**, 137–158.
25 D. De Vos, M. De Chial, C. Cochez, S. Jansen, B. Tümmler, J. M. Meyer and P. Cornelis, *Arch. Microbiol.*, 2001, **175**, 384–388.
26 E. E. Smith, D. G. Buckley, Z. Wu, C. Saenphimmachak, L. R. Hoffman, D. A. D'Argenio, S. I. Miller, B. W. Ramsey, D. P. Speert, S. M. Moskowitz, J. L. Burns, R. Kaul and M. V. Olson, *Proc. Natl. Acad. Sci. U. S. A.*, 2006, **103**, 8487–8492.
27 D. Nguyen and P. K. Singh, *Proc. Natl. Acad. Sci. U. S. A.*, 2006, **103**, 8305–8306.
28 J. Smith, J. D. Van Dyken and P. C. Zee, *Science*, 2010, **328**, 1700–1703.
29 A. S. Griffin, S. A. West and A. Buckling, *Nature*, 2004, **430**, 1024–1027.
30 J. E. Keymer, P. Galajda, G. Lambert, D. Liao and R. H. Austin, *Proc. Natl. Acad. Sci. U. S. A.*, 2008, **105**, 20269–20273.
31 B. Crespi, K. Foster and F. Úbeda, *Philos. Trans. R. Soc., B*, 2014, **369**, 20130366.
32 A. Buckling, F. Harrison, M. Vos, M. A. Brockhurst, A. Gardner, S. A. West and A. Griffin, *FEMS Microbiol. Ecol.*, 2007, **62**, 135–141.
33 R. Kümmerli, A. Gardner, S. A. West and A. S. Griffin, *Evolution*, 2009, **63**, 939–949.
34 M. A. Brockhurst, *PLoS One*, 2007, **2**, e634.
35 J. S. Chuang, O. Rivoire and S. Leibler, *Science*, 2009, **323**, 272–275.
36 P. B. Rainey and K. Rainey, *Nature*, 2003, **425**, 72–74.
37 C. D. Nadell, J. B. Xavier and K. R. Foster, *FEMS Microbiol. Rev.*, 2009, **33**, 206–224.
38 S. Park, P. M. Wolanin, E. A. Yuzbashyan, P. Silberzan, J. B. Stock and R. H. Austin, *Science*, 2003, **301**, 188.
39 S. Park, P. M. Wolanin, E. A. Yuzbashyan, H. Lin, N. C. Darnton, J. B. Stock, P. Silberzan and R. Austin, *Proc. Natl. Acad. Sci. U. S. A.*, 2003, **100**, 13910–13915.
40 A. Groisman, C. Lobo, H. Cho, J. K. Campbell, Y. S. Dufour, A. M. Stevens and A. Levchenko, *Nat. Methods*, 2005, **2**, 685–689.
41 H. Cho, H. Jönsson, K. Campbell, P. Melke, J. W. Williams, B. Jedynak, A. M. Stevens, A. Groisman and A. Levchenko, *PLoS Biol.*, 2007, **5**, e302.
42 Q. Zhang, G. Lambert, D. Liao, H. Kim, K. Robin, C. Tung, N. Pourmand and R. H. Austin, *Science*, 2011, **333**, 1764–1767.
43 A. K. Wessel, T. A. Arshad, M. Fitzpatrick, J. L. Connell, R. T. Bonnecaze, J. B. Shear and M. Whiteley, *MBio*, 2014, **5**, e00992.
44 R. H. Austin, C.-K. Tung, G. Lambert, D. Liao and X. Gong, *Chem. Soc. Rev.*, 2010, **39**, 1049–1059.
45 E. K. Sackmann, A. L. Fulton and D. J. Beebe, *Nature*, 2014, **507**, 181–189.
46 J. M. Meyer, A. Neely, A. Stintzi, C. Georges and I. A. Holder, *Infect. Immun.*, 1996, **64**, 518–523.
47 S. A. West and A. Buckling, *Proc. Biol. Sci.*, 2003, **270**, 37–44.
48 Y. Xia and G. M. Whitesides, *Annu. Rev. Mater. Sci.*, 1998, **28**, 153–184.
49 T. B. Doyle, A. C. Hawkins and L. L. McCarter, *J. Bacteriol.*, 2004, **186**, 6341–6350.
50 J. L. Connell, A. K. Wessel, M. R. Parsek, A. D. Ellington, M. Whiteley and J. B. Shear, *MBio*, 2010, **1**, e00202–00210.
51 K. Held, E. Ramage, M. Jacobs, L. Gallagher and C. Manoil, *J. Bacteriol.*, 2012, **194**, 6387–6389.
52 D. G. Davies, M. R. Parsek, J. P. Pearson, B. H. Iglewski, J. W. Costerton and E. P. Greenberg, *Science*, 1998, **280**, 295–298.
53 M. K. Brannon, J. M. Davis, J. R. Mathias, C. J. Hall, J. C. Emerson, P. S. Crosier, A. Huttenlocher, L. Ramakrishnan and S. M. Moskowitz, *Cell. Microbiol.*, 2009, **11**, 755–768.
54 T. Killingback, M. Doebeli and C. Hauert, *Biol. Theory*, 2010, **5**, 3–6.
55 G. Hardin, *Science*, 1968, **162**, 1243–1248.
56 B. J. Cardinale, J. P. Wright, M. W. Cadotte, I. T. Carroll, A. Hector, D. S. Srivastava, M. Loreau and J. J. Weis, *Proc. Natl. Acad. Sci. U. S. A.*, 2007, **104**, 18123–18128.
57 S. A. Levin and S. W. Pacala, in *Spatial ecology: the role of space in population dynamics and interspecific interactions*, ed. D. Tilman and P. Kareiva, Princeton University Press, Princeton, NJ, 1997, pp. 271–296.
58 S. A. Levin, *Bioscience*, 2005, **55**, 1075–1079.
59 M. W. Toepke and D. J. Beebe, *Lab Chip*, 2006, **6**, 1484–1486.
60 L. Yang, M. Nilsson, M. Gjermansen, M. Givskov and T. Tolker-Nielsen, *Mol. Microbiol.*, 2009, **74**, 1380–1392.
61 G. Bell and A. Gonzalez, *Science*, 2011, **332**, 1327–1330.
62 I. Hanski, *Nature*, 1998, **396**, 41–49.
63 A. Gonzalez, J. Lawton, F. Gilbert, T. Blackburn and I. Evans-Freke, *Science*, 1998, **281**, 2045–2047.
64 E. I. Damschen, L. A. Brudvig, N. M. Haddad, D. J. Levey, J. L. Orrock and J. J. Tewksbury, *Proc. Natl. Acad. Sci. U. S. A.*, 2008, **105**, 19078–19083.
65 P. D. Taylor, T. Day and G. Wild, *Nature*, 2007, **447**, 469–472.
66 S. Kéfi, M. van Baalen, M. Rietkerk and M. Loreau, *Am. Nat.*, 2008, **172**, E1–17.
67 M. A. Leibold, M. Holyoak, N. Mouquet, P. Amarasekare, J. M. Chase, M. F. Hoopes, R. D. Holt, J. B. Shurin, R. Law, D. Tilman, M. Loreau and A. Gonzalez, *Ecol. Lett.*, 2004, **7**, 601–613.